Acta Polytechnica CTU Proceedings **57**:226–238, 2026
https://doi.org/10.14311/APP.2026.57.0226
© 2026 The Author(s). Licensed under a CC-BY 4.0 licence
Published by the Czech Technical University in Prague

IMPACTS OF WATER DEPTH ON PEDESTRIAN SPEED, GAIT, AND STABILITY: RESULTS FROM AN EXPERIMENTAL STUDY

Xintong Li[a, b], Weiguo Song[a,*], Jun Zhang[a], Nikolai W.F. Bode[b]

[a] *University of Science and Technology of China, State Key Laboratory of Fire Science, 230027 Hefei, China*

[b] *University of Bristol, School of Engineering Mathematics and Technology, BS8 1TW Bristol, UK*

[*] corresponding author: wgsong@ustc.edu.cn

Abstract. Under rapid socio-economic development and increasingly frequent extreme weather events, flood disasters have led to growing losses and casualties, highlighting the importance of understanding pedestrian dynamics in flooded environments. This study conducted controlled movement experiments involving 188 participants across four water depths (0, 0.35, 0.60, and 0.90 m) to investigate the effects of water depth on walking behavior. Results show that water depth significantly influences pedestrian speed and gait characteristics. When depth increased from 0 m to 0.35 m, pedestrian speed decreased by 38.6 % for males and 44.8 % for females, lateral swaying amplitude increased by 69 % and 133.3 %, and step length shortened by 37.0 % and 32.0 %, respectively. Further increases in depth resulted in progressively smaller changes. Water also exacerbated gender differences in walking speed, while disparities in stride frequency, step length, and swaying amplitude were most pronounced under dry conditions. At depths up to 0.90 m, the coefficients of variation for step length and stride frequency increased, indicating diminished gait stability. These findings clarify how water depth affects pedestrian movement and stability, reveal gender-specific behavioral responses, and provide essential empirical data to improve flood evacuation modeling and enhance pedestrian safety during flood events.

Keywords: Flood evacuation, evacuation experiment, pedestrian dynamics, walking speed, gait characteristics.

1. Introduction

The intensification of human activities, coupled with the increasing frequency of extreme weather events, has substantially elevated the risk of urban flooding [1]. Rapid urbanization has transformed the surface environment of cities, as high-density construction and extensive road paving impose heavy demands on drainage systems, often leading to flooding events such as waterlogging and infrastructure leakage. Urban flooding now represents a major threat to public safety and property, posing critical challenges to the sustainable development of cities worldwide [2, 3].

With the rapid development of society and the economy, flood-related economic losses and casualties have intensified [4], drawing substantial academic interest. Numerical flood simulations, grounded in historical disaster data [5] and geographic information systems [6]], serve as valuable tools for disaster prediction and preparedness. In the event of a disaster, effective evacuation strategies are essential for reducing casualties. Therefore, many researchers have developed regional evacuation models aimed at optimizing evacuation methods and identifying the most effective evacuation routes [7–9]. Meanwhile, an increasing number of microscopic models have been developed to simulate pedestrian movement during evacuations [10–13], offering deeper insights into pedestrian dynamics and facilitating the refinement of flood evacuation strategies.

Human instability represents a critical factor contributing to flood-related casualties. Recent studies have investigated the mechanisms underlying human instability in floodwaters, establishing criteria for its onset through flume experiments [14, 15], mechanical analyses [16, 17] across various scales, and integrated approaches combining both methods [18]. These studies consider a wide range of human characteristics [19] and postures [15], as well as hydrodynamic conditions [20]. Findings indicate that human instability arises from two primary physical mechanisms: moment instability (tipping) and friction instability (slipping) [21]. Building on this, subsequent research has derived equations for predicting the initial flow velocity required to trigger instability based on mechanical principles [18] and has identified specific thresholds of water depth and flow velocity that pose instability risks, as informed by flume tests [15, 17, 22]. Additionally, criteria linking instability to individual human characteristics have been formulated to improve predictive accuracy [19].

Research on pedestrian movement characteristics has received increasing attention, as pedestrian motion is influenced by diverse factors, including individual traits, environmental conditions, and interactions with floodwaters [23–25]. However, studies on pedestrian movement in flood conditions remain limited due to experimental constraints. Ishigaki et al. [26] conducted tank tests on 99 participants (83 males and 16 females), revealing that walking speed declined

as water depth increased from 0 to 0.5 m, eventually reducing to half of the speed observed in normal conditions at a depth of 0.5 m. Lee et al. [27] conducted experiments with 32 participants (20 males and 12 females) who wore geriatric simulators to imitate the movement of older adults in water depths ranging from 0 to 0.5 m. The results showed that both walking and running speeds decreased as water depth increased, with a minimal difference in speeds between genders. The decrease in speed was particularly significant when the water depth increased from 0 to 0.1 m. Bernardini et al. [25] assessed the walking and running speeds of 203 volunteers aged 8 to 68 years across water depths of 0.2 to 0.7 m. They observed a speed decline with increasing water depth, noting an inverse relationship between speed and specific characteristics such as age, height, weight, and BMI, with females exhibiting higher speeds than males. Dias et al. [28] tested 14 volunteers (6 males and 8 females) at three water depths (0.08 m, 0.43 m, and 0.90 m), measuring body sway amplitude and stride frequency through trajectory analysis. Their findings indicated a consistent decrease in speed as water depth increased, with male participants exhibiting significantly higher speeds than females at 0.90 m. Furthermore, trajectory analysis showed that body sway amplitude increased, while stride frequency decreased in flooded conditions compared to normal conditions.

Empirical data on pedestrian behavior serve as the foundation for the development, calibration, and validation of evacuation models. A comprehensive understanding of pedestrian movement speed and behavioral patterns in flood scenarios is crucial for optimizing flood evacuation strategies, thereby enhancing emergency response plans and minimizing casualties. However, existing research has yet to reach a consensus regarding the impact of gender on movement speed, and there remains a paucity of data on pedestrian gait characteristics. To address this gap, the present study conducted experiments to examine pedestrian movement at four distinct water depths (0 m, 0.35 m, 0.60 m, and 0.90 m), representing no water, below-knee, above-knee, and waist-high water conditions. The objective was to elucidate the effects of gender and water depth on pedestrian speed, uncover gait characteristics at varying water depths, and contribute richer data on pedestrian movement dynamics. The remainder of this paper is organized as follows. Section 2 outlines the experimental setup, Section 3 presents the experimental results and compares them with previous studies, and Section 4 provides a summary and discussion of the findings.

2. Experiment setup

This controlled experiment was conducted in July 2024 at the University of Science and Technology of China. The experimental protocols were reviewed and approved by the institutional ethics committee (No. 2024-N(H)-317).

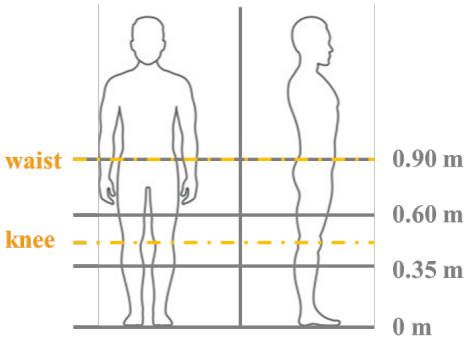


Figure 1. Schematic of experimental water depths. 4 solid gray lines represent the 4 experimental water depths, and two orange dotted lines represent waist and knee heights.

2.1. Experimental environment

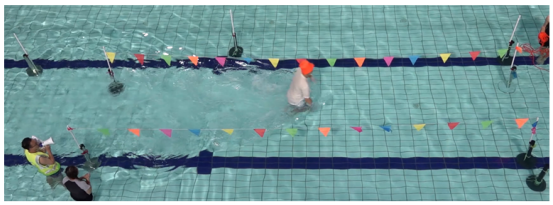
Water depths for the experiment were determined based on the Human dimensions of Chinese adults [29], corresponding to four levels: 0.90 m (waist height), 0.60 m (above the knee), 0.35 m (below the knee), and 0 m. Figure 1 presents schematic diagrams illustrating each experimental water depth. In-water trials were performed in a swimming pool under controlled conditions, maintaining a water temperature of 26 °C, standard water density, clear water free of sediment or silt, and no currents, other than those induced by the movement of participants. Experiments for the no-water condition (0 m depth) were carried out in an open area in front of the university building.

2.2. Participant characteristics

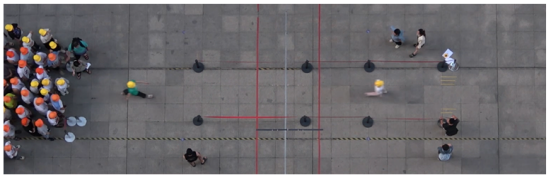
The experiment involved 188 student volunteers (101 males and 87 females) aged 16 to 33 years, with an average age of 22.3 ± 3.5 years, an average height of 1.7 ± 0.1 m, and an average weight of 62.6 ± 12.0 kg. The experiments for the four water depths were completed over two days, with specific participant details as follows: 114 volunteers (74 males and 40 females) participated in the 0.90 m water depth experiment on July 29th at 2 PM; 97 volunteers (53 males and 42 females) in the 0.60 m depth on July 30th at 9 AM; 133 volunteers (70 males and 63 females) in the 0.35 m depth on July 30th at 2 PM; and 88 volunteers (54 males and 34 females) in the no-water (0 m) condition on July 30th at 5 PM.

2.3. Experimental procedure and data extraction

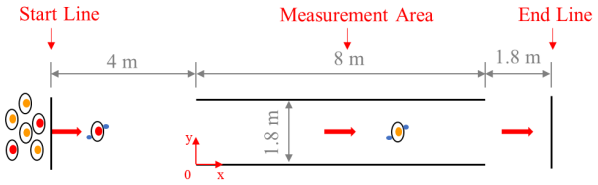
The experiment was conducted within a 1.8 m wide and 8 m long channel delineated by guard poles. Figure 2 illustrates the experimental setup: Figure 2a presents a video frame from the in-water experiment, Figure 2b shows a frame from the on-land (0 m depth) experiment, and Figure 2c provides a schematic of the experimental layout. Prior to each trial, participants gathered on the left side of the Start Line. Upon the start signal, each volunteer began from the Start Line,



(A). A video frame from the in-water experiment.



(B). A frame from the on-land (0 m depth) experiment.



(C). A schematic of the experimental layout.

Figure 2. Experimental layout.

simulating an emergency evacuation by proceeding quickly and safely through the measurement area to the End Line. To prevent interference, each volunteer was tested individually. After the current volunteer completed their traversal of the measurement area and left the corridor, the next volunteer would then begin their test.

To facilitate trajectory data extraction, male participants wore orange hats, while female participants wore red hats. Volunteers walked barefoot and wore common clothes during the water experiments (a few participants wore swimsuits), and wore shoes for the on-land condition. A camera recorded the entire experiment at 25 fps with a resolution of 1920×1080 pixels. *Petrack* software [30] was used to calibrate the video, converting 2D pixel coordinates into real-world 3D coordinates. The average error for the present dataset was less than 0.02 m.

3. Results

3.1. Trajectories and pedestrian behavior

Pedestrian trajectories within the measurement area ($0 \leq x \leq 8\,\text{m}, 0 \leq y \leq 1.8\,\text{m}$) were extracted using *Petrack* software [30]. Figure 3 displays the trajectories across varying water depths.

The color variations indicate that pedestrian speed remains relatively steady within the 8 m measurement range but decreases progressively with increasing water depth. Trajectory comparisons between land and water conditions reveal more pronounced fluctuations in water, suggesting that pedestrians increase body sway to maintain balance in water conditions.

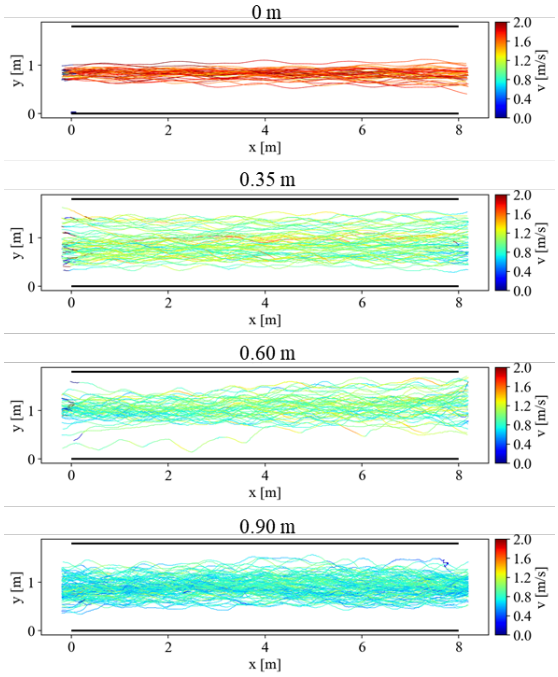


Figure 3. Pedestrian trajectories across different water depths, with the color bar indicating instantaneous speed (see Appendix A.1). From top to bottom, the trajectories correspond to water depths of 0 m, 0.35 m, 0.60 m, and 0.90 m, respectively.

Experimental video observations show that pedestrians exhibit different behavioral characteristics when walking in water than on land. Pedestrians increased their arm-swing amplitude to better maintain balance in water relative to land. Under the 0.90 m water depth condition, some pedestrians also assisted their movement by paddling with their arms (see Figure 4), which helped reduce water resistance, enhance propulsion, and improve stability. In addition, pedestrians displayed a range of gaits in water, including regular strides and mini-strides, with no instances of foot-lifting above the water surface, even in shallow depths (0.35 m). This gait adaptation likely results from the combined effects of buoyancy and drag, which cause pedestrians to reduce leg lift to lower drag and conserve energy. The shortened stride length and limited leg-lifting motion contribute to more efficient movement in water.

3.2. Speed

The pedestrian movement speed was defined as the mean instantaneous speed within the Measurement Area ($0 \leq x \leq 8\,\text{m}$). Given that speed distributions at each water depth did not follow a normal distribution, the Interquartile Range (IQR) method was applied to represent speed statistics. Table 1 presents the minimum, $Q1$, median, $Q3$, maximum, and IQR values ($IQR = Q3 - Q1$) of movement speeds for the total sample, as well as for male and female participants at each water depth, along with corresponding sample sizes, means, and standard deviations.

Speed [m s^{-1}]	Water depth [m]											
	0.90			0.60			0.35			0		
	All	Male	Female	All	Male	Female	All	Male	Female	All	Male	Female
Min	0.50	0.68	0.50	0.63	0.75	0.63	0.63	0.67	0.63	1.22	1.22	1.22
Q1	0.72	0.78	0.62	0.78	0.88	0.73	0.85	0.93	0.81	1.55	1.58	1.52
Median	0.78	0.82	0.69	0.89	1.00	0.77	0.96	1.06	0.87	1.69	1.73	1.62
Q3	0.86	0.89	0.75	1.00	1.07	0.87	1.11	1.15	1.00	1.80	1.82	1.73
Max	1.08	1.08	0.90	1.49	1.49	1.08	1.86	1.86	1.23	2.91	2.15	2.91
IQR	0.14	0.11	0.13	0.22	0.19	0.14	0.26	0.22	0.19	0.25	0.24	0.21
Sample dimension	114	74	40	95	53	42	133	70	63	88	54	34
Mean	0.79	0.84	0.68	0.91	1.00	0.80	0.99	1.05	0.91	1.69	1.71	1.65
std	0.12	0.09	0.09	0.16	0.15	0.11	0.18	0.19	0.14	0.23	0.20	0.28

TABLE 1. Statistical characterization of pedestrian speed at different water depths.

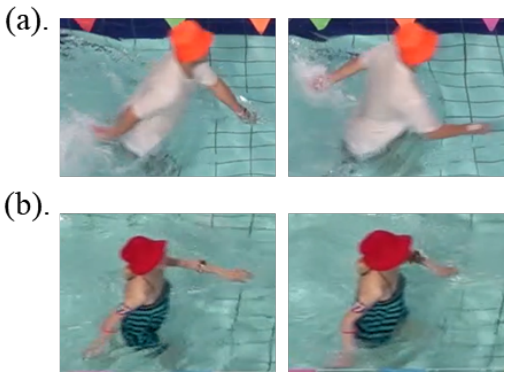


FIGURE 4. Arm-assisted walking patterns of pedestrians observed at a water depth of 0.90 m. (a) shows a male participant employing arm paddling for balance and propulsion, while (b) captures a similar pattern in a female participant.

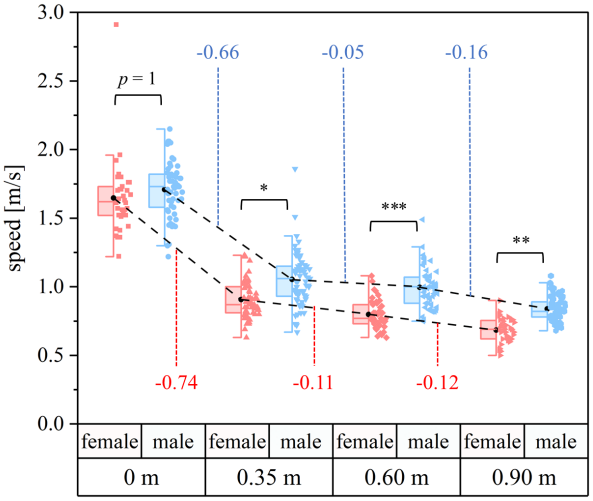


FIGURE 5. Boxplot of pedestrian movement speeds by gender across water depths. The left side of the box-and-whisker plot displays the interquartile range for movement speeds, while the right side shows the scatter distribution. Blue dashed lines and numerical labels represent changes in male speeds across adjacent water depths, while red markings indicate female speeds. *Dunn's post-hoc test* significance markers are also included: *** for p < 0.001, ** for p < 0.01, and * for p < 0.05, denoting significant differences across water depths.

First, Pearson correlation analysis was conducted to examine the relationships between height, weight, and pedestrian walking speed (see A.2). The results indicate that, under all three water depth conditions, both height and weight are significantly positively correlated with walking speed ($p < 0.05$). However, the correlation coefficients r are all below 0.4, suggesting that the overall correlations are relatively weak. Based on this, a multiple linear regression analysis was further performed, in which height, weight, gender, and water depth were included as explanatory variables. The results show that gender ($p < 0.001$) and water depth ($p < 0.001$) are the primary factors influencing walking speed, whereas height ($p = 0.835$) and weight ($p = 0.597$) are no longer statistically significant after controlling for other variables, indicating that their effects on walking speed are limited.

These findings suggest that the influence of anthropometric characteristics on walking speed is limited. Therefore, greater attention is given in the following to the effects of water depth and gender on pedestrian movement.

3.2.1. EFFECT OF WATER DEPTH AND GENDER ON SPEED

Figure 5 presents male and female movement speeds at varying water depths. Overall, a declining trend in walking speed is evident for both genders as water depth increases. Notably, when water depth rose from 0 m to 0.35 m, pedestrian speeds dropped significantly, with average male speeds decreasing by 0.66 m s^{-1} (38.6 %) and average female speeds by 0.74 m s^{-1} (44.8 %). Beyond 0.35 m, as depth increased to 0.60 m and 0.90 m, the rate of speed reduction leveled off, suggesting that while the presence of water substantially impacts pedestrian speed, additional depth increases exert a diminishing influence.

Additionally, by examining the boxplots in Figure 5 alongside the IQR values in Table 1, we observe that IQR values decline as water depth increases. This indicates reduced data dispersion with increasing depth, implying that deeper water not only slows pedestrian speeds but also minimizes speed variation within each gender group.

The *Kruskal–Wallis H-test* revealed significant differences in pedestrian speed across gender–water depth groups ($\chi^2 = 308.95$, DF $= 7$, $p < 0.001$), indicating a combined effect of gender and water depth. *Dunn's post-hoc* analysis (see Appendix A.2) showed no significant gender difference at 0 m depth ($p = 1$), while significant differences were observed at other depths ($p < 0.001$).

3.2.2. Comparison with previous studies

The mean and standard deviation were utilized to represent pedestrian speed data in this experiment, allowing for direct comparison with previous studies (see Figure 6). Characteristics of the comparative data illustrated in Figure 6 are detailed in Table 6 in Appendix A.2. Results indicate that the observed trend of decreasing pedestrian speed with increasing water depth in this study aligns well with prior findings. Specifically, in this study, a notable reduction in speed was observed as water depth rose from 0 m to 0.35 m, aligning with the trend reported by Lee et al. [27] for depths between 0 m and 0.2 m. At greater depths (0.35 m to 0.90 m), the rate of speed reduction diminished, a trend also noted by Lee et al. [27] (0.2 m to 0.5 m) and supported by findings from Dias et al. [28] and Bernardini et al. [25]. This further indicates a potential nonlinear effect of water depth on pedestrian speed.

In this study, pedestrian speeds were slightly higher, likely reflecting differences in experimental settings, cultural background, and participant characteristics. A noteworthy finding was a significant gender difference in water walking speeds. Although Bernardini et al. [25] reported a statistically significant gender effect, the magnitude of the difference in their data was relatively small and not visually evident. This discrepancy may be due to differences in experimental motivation. In our study, participants were instructed to walk as fast as possible while maintaining safety, which may enhance performance and amplify gender-related differences. Furthermore, Dias et al. [28] and Lee et al. [27] included smaller sample sizes, while Bernardini et al. [25], though they had a larger sample size, included a broader age range and did not analyze speed differences by gender within the same age group.

The specific flood forces M (see Appendix A.1) associated with water depths of 0.90 m, 0.60 m, and 0.35 m in this study were 0.405 $m^3\,m^{-1}$, 0.18 $m^3\,m^{-1}$ and 0.06 $m^3\,m^{-1}$, respectively. The relationship between the pedestrian speed in water v_i, and the specific flood force was fitted using Eq. 3 in Appendix A.1. Similarly, the relationship between the minimum observed speed v_{min}, and the specific flood force (as shown in Table 7 in Appendix A.2) was fitted. Figure 7 presents a comparison of these fitted curves with previous studies [25, 28]. Results indicate that the fitted mean speed curve for the current experiment exceeds those reported by Dias et al. [28] and Bernardini et al. [25], likely reflecting differences in experimental protocols, participant characteristics, and cultural factors. Table 6 in Appendix A.2 provides parameter values for these fitted curves, alongside data on sample characteristics.

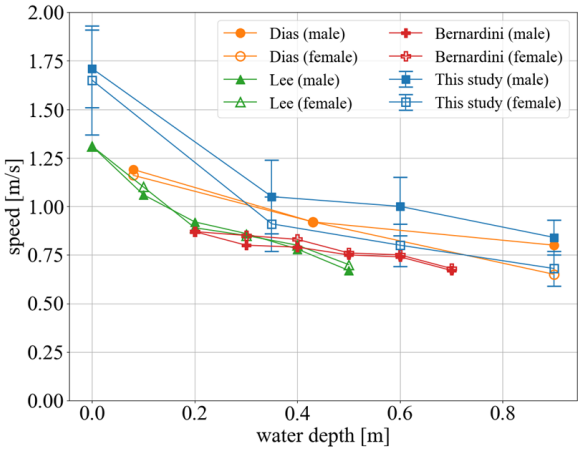


Figure 6. Comparison with previous studies.

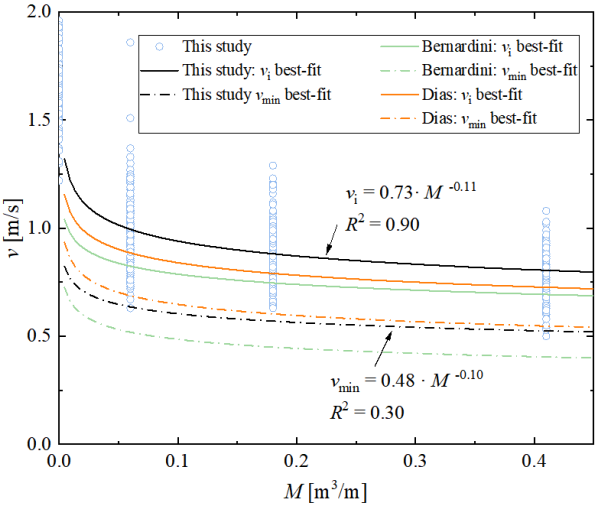


Figure 7. Comparison of $M - v_i$ characteristics.

3.3. Lateral swaying

3.3.1. Effect of water depth and gender on the lateral swaying amplitude

Lateral swaying amplitudes of pedestrian trajectories were measured across various water depths and summarized in Figure 8. Each data point represents the average amplitude of a pedestrian's lateral swaying within the measurement area ($0 \leq x \leq 8$ m). The findings indicate a significant gender difference in lateral swaying amplitudes at 0 m water depth

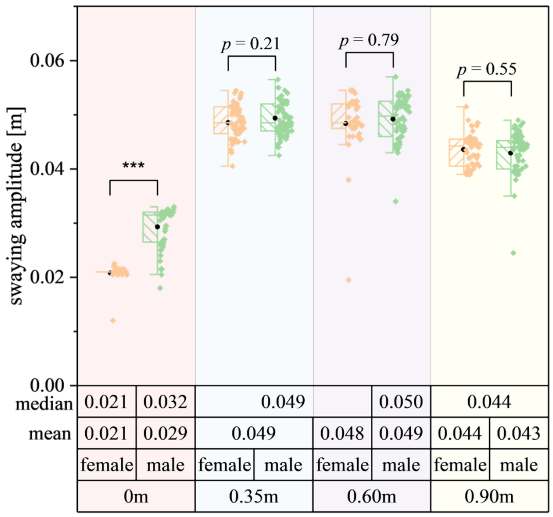


FIGURE 8. Grouped box plots illustrating lateral swaying amplitudes by gender. *Kruskal-Wallis* test results assessing the effect of gender on lateral swaying amplitudes at each water depth are indicated in the figure, with "***" denoting $p < 0.001$, signifying a statistically significant difference.

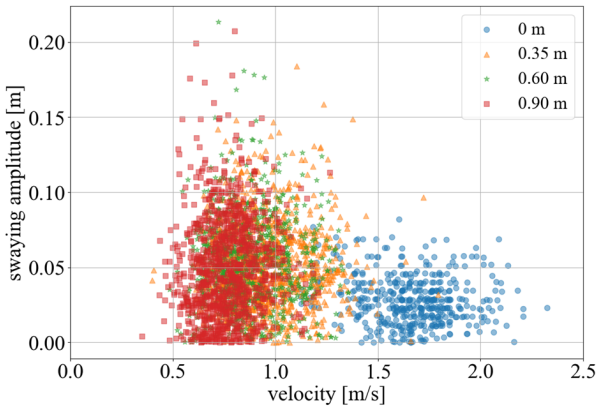


FIGURE 9. Scatter plots of pedestrian velocity versus lateral swaying amplitude across varying water depths.

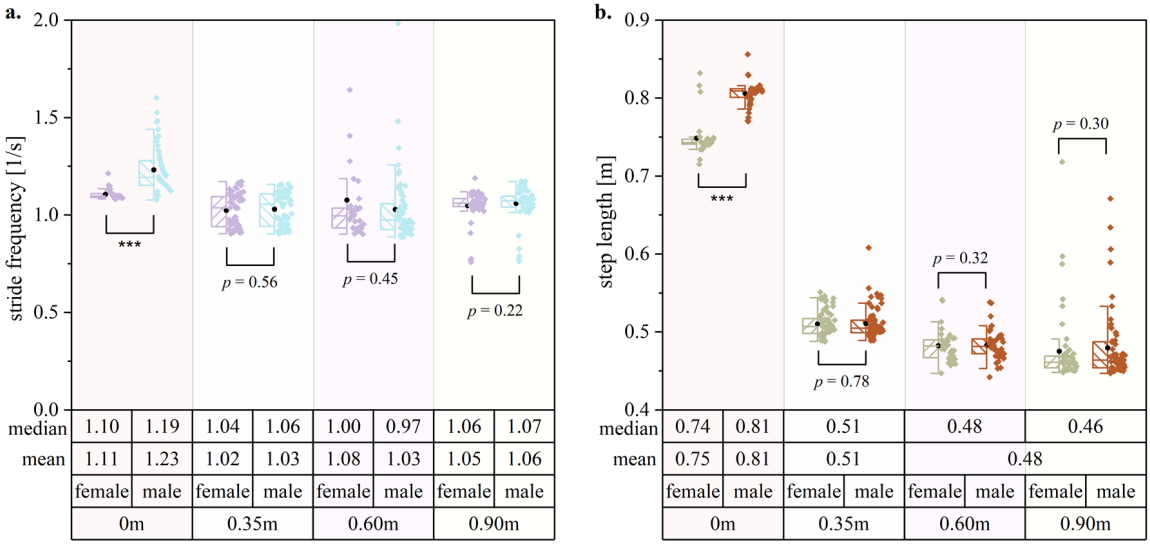
($\chi^2 = 53.47,\ p < 0.0001$), with no such difference detected at other depths. This pattern suggests that, under normal conditions, females tend to maintain greater body stability during walking, whereas males exhibit relatively larger lateral body movements because of a more expressive walking style. In water, however, the combined effects of resistance and buoyancy necessitate greater lateral swaying for balance, thereby reducing the sensitivity of lateral swaying to gender differences.

No positive correlation was observed between water depth and the amplitude of pedestrians' lateral swaying. Lateral swaying amplitude increased significantly when water depth increased from 0 m to 0.35 m, with an average increase of 69 % for males and 133.3 % for females. Swaying amplitude was highest at water depths of 0.35 m and 0.60 m, followed by 0.90 m. This lateral swaying amplitude indicates pedestrians' lateral stability during walking: at 0 m depth, pedestrians required minimal body sway to maintain balance. However, at depths of 0.35 m and 0.60 m, where the lower body was partially submerged, a greater lateral swaying was necessary to maintain stability, resulting in increased swaying amplitude. At 0.90 m, as the legs were fully submerged and constrained by the current, the water provided additional support, enhancing stability and reducing lateral swaying amplitude. A *Kruskal-Wallis* test confirmed that water depth significantly affected lateral swaying amplitude ($\chi^2 = 293.86,\ DF = 3,\ p < 0.0001$). *Dunn's post-hoc* test (Table 5 in Appendix A.2) indicated no significant difference between swaying amplitudes at 0.35 m and 0.60 m depths, while significant differences were observed between all other depths. These findings suggest that water depths of 0.35 m and 0.60 m may create similar resistance and support conditions, yielding comparable sway dynamics.

Figure 9 presents scatter plots of pedestrian velocity (in the x direction) versus lateral swaying amplitude across varying water depths. Unlike the linear relationships identified in prior study [31], no significant linear correlation was detected in this study. Spearman correlation tests indicated limited statistically significant associations only at 0 m and 0.90 m water depths, both of which were weak: a slight negative correlation was observed at 0 m ($Spearman\ Corr. = -0.12,\ p = 0.01$), while a slight positive correlation was observed at 0.90 m ($Spearman\ Corr. = 0.1,\ p = 0.002$). No significant correlation was found at 0.35 m and 0.60 m water depths (p-values of 0.90 and 0.73, respectively), suggesting minimal association between velocity and lateral swaying amplitude. Overall, the findings did not indicate a significant correlation between pedestrian velocity and lateral swaying amplitude.

3.3.2. EFFECT OF WATER DEPTH AND GENDER ON STRIDE FREQUENCY AND STEP LENGTH

Figure 10 presents box plots of stride frequency and step length at different water depths, with *Kruskal–Wallis test* results annotated in the figure. The analysis shows that gender differences in stride frequency ($\chi^2 = 46.8,\ p < 0.0001$) and step length ($\chi^2 = 46.2,\ p < 0.0001$) are significant only at 0 m water depth. Additionally, water depth significantly affects both stride frequency ($\chi^2 = 133.4,\ DF = 3,\ p < 0.0001$) and step length ($\chi^2 = 306.0,\ DF = 3,\ p < 0.0001$). Overall, pedestrian stride frequency remains around 1 Hz across all water depths, while step length decreases significantly as water depth increases: at 0 m water depth, the average step lengths for females and males are 0.75 m and 0.81 m, respectively; at 0.35 m, 0.60 m, and 0.90 m water depths, step lengths decrease to 0.51 m, 0.48 m, and 0.46 m, respectively. These results indicate that the increase in water depth primarily affects the reduction of step length, rather than stride frequency. Furthermore,



	0m		0.35m		0.60m		0.90m	
median	1.10	1.19	1.04	1.06	1.00	0.97	1.06	1.07
mean	1.11	1.23	1.02	1.03	1.08	1.03	1.05	1.06
	female	male	female	male	female	male	female	male

	0m		0.35m		0.60m		0.90m	
median	0.74	0.81	0.51		0.48		0.46	
mean	0.75	0.81	0.51		0.48			
	female	male	female	male	female	male	female	male

Figure 10. (a). Pedestrian stride frequency at each water depth; (b). Pedestrian step length at each water depth. The results of the *Kruskal–Wallis test* assessing the effect of gender on stride frequency and step length at each water depth are indicated in the figure, with *** denoting a significant difference ($p < 0.001$).

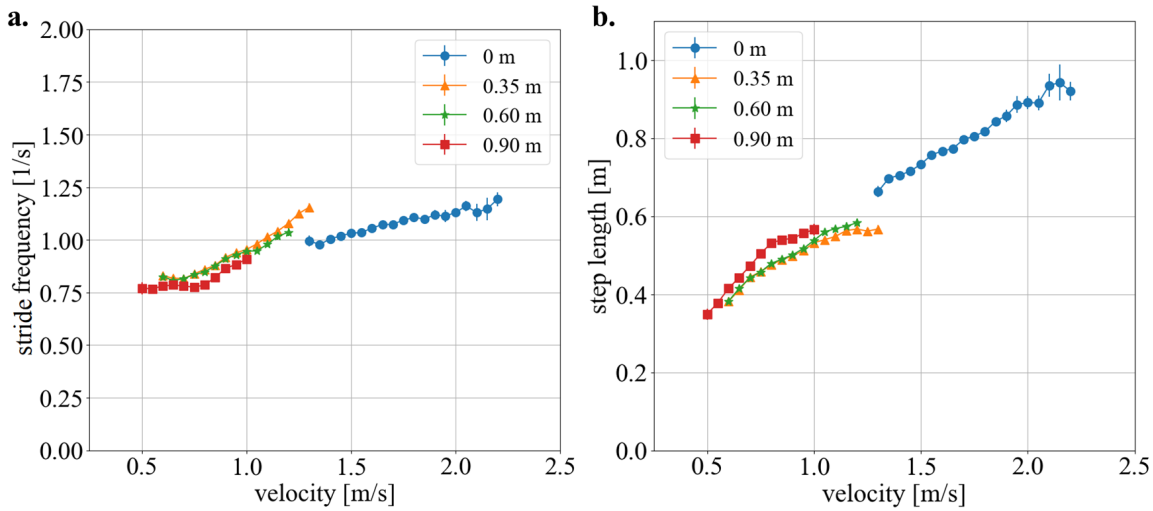


Figure 11. (a). Relationship between stride frequency and velocity in the direction of motion for different water depths; (b). Relationship between step length and velocity in the direction of motion for different water depths.

the smaller variation in step length between 0.35 m and 0.90 m water depths explains the relatively small reduction in speed within this range.

Figure 11 illustrates the relationship between stride frequency, step length, and velocity in the direction of motion across different water depths. At 0 m water depth, both stride frequency and step length exhibit a clear linear correlation with velocity, such that increases in velocity are accompanied by proportional increases in step length and stride frequency. However, at the other three water depths, the relationship between gait characteristics and velocity varies. At lower velocities ($v_x < 0.75\,\mathrm{m\,s^{-1}}$), an increase in velocity is primarily achieved through an increase in step length. As velocity continues to rise, both step length and stride frequency increase concurrently. Notably, when step length reaches approximately 0.55 m, the primary mechanism for further velocity increases shifts, with stride frequency becoming the predominant factor driving speed enhancement.

We introduce the coefficient of variation (CV) (see Appendix A.1)as a measure of the stability of stride frequency and step length during walking. A lower CV value indicates greater consistency and smaller fluctuations in the measured parameters. The CVs for step length and stride frequency were calculated for each pedestrian in the measurement area. Figure 12 presents box plots of the CVs for stride frequency and step length across four water depths. The analysis reveals significant differences in the CVs for both stride frequency and step length under varying water depth conditions. The CVs for both parameters were lower in the no-water (0 m) and shallower water depths (0.35 m and 0.60 m), suggesting a more stable gait.

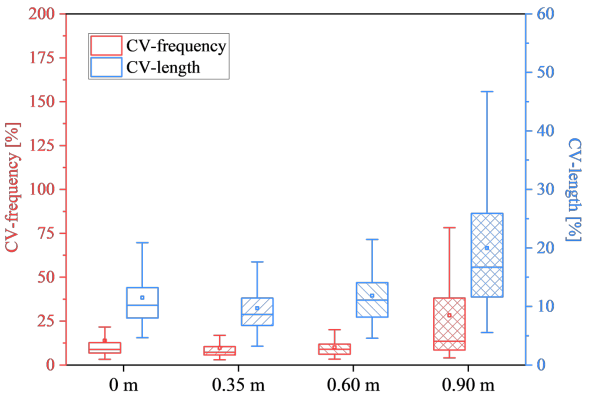


FIGURE 12. Boxplots of coefficient of variation for step length and stride frequency. The red box plot represents the coefficient of variation of stride frequency ($CV_{frequency}$), which corresponds to the left red axis, and the blue box plot represents the coefficient of variation of step length (CV_{length}), which corresponds to the right blue axis. The box in the boxplot shows the middle 50 % of the data, with the lower and upper edges representing the 25th and 75th percentiles. The line inside the box shows the median value, which is the middle point of the data. The whiskers extend from the box to show the range of the data, excluding extreme values. The mean is marked with a circle, showing the average value.

However, as the water depth increased to 0.90 m, there was a marked increase in the CV of step length, and a corresponding increase in the CV of stride frequency, indicating a reduction in gait stability. These findings suggest that deeper water depths introduce greater perturbations to pedestrian gait, leading to higher variability in both step length and stride frequency.

4. Discussion and conclusion

In the context of emergency evacuations and rescue operations during flooding events, both affected individuals and rescuers frequently encounter the necessity of traversing through water. Consequently, a thorough understanding of pedestrian dynamics in flood environments is imperative for ensuring the safety of evacuees. This study selected four experimental water depths, 0.90 m (waist height), 0.60 m (above knee height), 0.35 m (below knee height), and 0 m (no water), to investigate pedestrian movement behaviors among college students with an average age of 22.3 ± 3.5 years. This study aims to explore variations in pedestrian movement speeds across different water depths and analyze gait characteristics in these conditions. The principal findings of this study are as follows:

(1) Water depth and gender significantly influenced pedestrian speeds, with a notable decline in speed as water depth increased. Specifically, pedestrian speeds decreased markedly (by 38.6 % for males and 44.8 % for females) when transitioning from 0 m to 0.35 m water depth, with further increases in water depth showing minimal additional decrease. Gender differences in speed were pronounced in water, revealing that female speeds were particularly sensitive to water depth changes. Analysis also indicated that increased water depth minimized speed variation within each gender group.

(2) Water depth plays a crucial role in pedestrian lateral stability. As water depth increased from 0 m to 0.35 m, lateral sway in pedestrians showed a marked increase, with mean amplitude rising by 69 % in males and 133.3 % in females. The greatest sway amplitudes were observed at water depths of 0.35 m and 0.60 m, followed by a decline at 0.90 m depth, suggesting a stabilization effect at deeper levels. Notably, a significant effect of gender on lateral sway amplitude was evident only at 0 m depth. No significant linear correlation was found between velocity and lateral sway amplitude, with only a weak correlation at 0 m and 0.90 m depths.

(3) Water depth significantly impacted step length, stride frequency, and gait stability. In shallow water, the coefficients of variation (CV) for both step length and stride frequency were low, indicating stable gait, whereas at 0.90 m depth, CVs increased, signifying a decline in gait stability and increased variability in step length and frequency. Furthermore, the impact of water depth was more pronounced on step length than on stride frequency, with reductions in pedestrian speed primarily attributed to shortened step lengths as water depth increased.

This study provides key insights into the variations in pedestrian movement speed and gait characteristics across different water depths, offering crucial empirical data for understanding the mechanisms governing locomotion in water. Compared with previous studies [25–28], this work involved a larger sample size, focused on a consistent age group, and found that the relationship between speed and water depth aligns with existing literature. The findings not only confirm the influence of water depth on pedestrian speed but also underscore the impact of gender in water movement and suggest a potential nonlinear relationship between water depth and speed. Furthermore, this research examines pedestrian dynamics in flood evacuation scenarios, contributing valuable data for use as model parameters in pedestrian movement simulation and flood risk analysis. Consistent with observations by Dias et al. [28], this study finds that lateral swaying amplitude is greater in water, suggesting that pedestrians increase body sway to maintain balance, thus requiring greater personal space. The gait data collected may also aid in the development of bipedal locomotion models. By introducing the coefficient of variation (CV) to quantify gait stability, this study reveals a decline in gait stability in deeper water depths, marking a novel approach to analyzing gait consistency in water environments. These findings hold valuable implications for flood evacuation modeling and the refinement of emergency response

strategies.

While this study provides valuable insights into pedestrian dynamics at varying water depths, several limitations must be acknowledged. First, the experimental environment was idealized and did not account for the effects of flowing water or small waves generated by pedestrian movement, which may influence ground visibility, both of which are common in real flood scenarios. Additionally, the sample consisted solely of college students, a relatively homogeneous group that may not fully represent broader demographic variations. Analyses were limited to pedestrian trajectory data and did not include potential psychological factors such as stress and fatigue.

To address these limitations, future research could incorporate more realistic conditions, including moving water, low-visibility scenarios, and interactions between walking direction and flow. Furthermore, integrating psychological and physiological factors, as well as expanding sample diversity and water depth conditions, would provide a more comprehensive understanding of pedestrian behavior in flood environments.

Acknowledgements

This study was supported by the National Natural Science Foundation of China (52574284), China Scholarship Council (No. 202306340073).

References

[1] P. Hu, Q. Zhang, P. Shi, et al. Flood-induced mortality across the globe: Spatiotemporal pattern and influencing factors. *Science of The Total Environment* **643**:171–182, 2018. https://doi.org/10.1016/j.scitotenv.2018.06.197

[2] J. Rentschler, P. Avner, M. Marconcini, et al. Global evidence of rapid urban growth in flood zones since 1985. *Nature* **622**:87–92, 2023. https://doi.org/10.1038/s41586-023-06468-9

[3] EM-DAT. The international disasters database. [2025-02-08]. https://www.emdat.be/

[4] S. Zhang, Z. Jing, W. Li, et al. Study of the flood control scheduling scheme for the Three Gorges Reservoir in a catastrophic flood. *Hydrological Processes* **32**(11):1625–1634, 2018. https://doi.org/10.1002/hyp.11515

[5] H. Takagi, S. Li, M. de Leon, et al. Storm surge and evacuation in urban areas during the peak of a storm. *Coastal Engineering* **108**:1–9, 2016. https://doi.org/10.1016/j.coastaleng.2015.11.002

[6] W. Zhang, J. Zhou, Y. Liu, et al. Emergency evacuation planning against dike-break flood: a GIS-based DSS for flood detention basin of Jingjiang in central China. *Natural Hazards* **81**:1283–1301, 2016. https://doi.org/10.1007/s11069-015-2134-7

[7] N. Wood, J. Jones, J. Peters, K. Richards. Pedestrian evacuation modeling to reduce vehicle use for distant tsunami evacuations in Hawai'i. *International Journal of Disaster Risk Reduction* **28**:271–283, 2018. https://doi.org/10.1016/j.ijdrr.2018.03.009

[8] M. Borowska-Stefańska, M. Kowalski, F. Turoboś, S. Wiśniewski. Optimisation patterns for the process of a planned evacuation in the event of a flood. *Environmental Hazards* **18**(4):335–360, 2019. https://doi.org/10.1080/17477891.2019.1593816

[9] Y. H. Lee, H. I. Kim, K. Y. Han, W. H. Hong. Flood evacuation routes based on spatiotemporal inundation risk assessment. *Water* **12**(8):2271, 2020. https://doi.org/10.3390/w12082271

[10] W. M. Cao, Shuchao, J. Ni, et al. Research on crowd movement characteristics and evacuation modeling in subway stations under flood disaster. *Journal of Railway Science and Engineering* pp. 1–11, 2023. https://doi.org/10.19713/j.cnki.43-1423/u.T20230119

[11] Y. Zheng, X.-G. Li, B. Jia, R. Jiang. Simulation of pedestrians' evacuation dynamics with underground flood spreading based on cellular automaton. *Simulation Modelling Practice and Theory* **94**:149–161, 2019. https://doi.org/10.1016/j.simpat.2019.03.001

[12] G. Bernardini, M. Postacchini, E. Quagliarini, et al. A preliminary combined simulation tool for the risk assessment of pedestrians' flood-induced evacuation. *Environmental Modelling & Software* **96**:14–29, 2017. https://doi.org/10.1016/j.envsoft.2017.06.007

[13] M. Shirvani, G. Kesserwani. Flood–pedestrian simulator for modelling human response dynamics during flood-induced evacuation: Hillsborough stadium case study. *Natural Hazards and Earth System Sciences* **21**(10):3175–3198, 2021. https://doi.org/10.5194/nhess-21-3175-2021

[14] Z. Zhu, Y. Zhang, L. Gou, et al. On the physical vulnerability of pedestrians in urban flooding: Experimental study of the hydrodynamic instability of a human body model in floodwater. *Urban Climate* **48**:101420, 2023. https://doi.org/10.1016/j.uclim.2023.101420

[15] E. Martínez-Gomariz, M. Gómez, B. Russo. Experimental study of the stability of pedestrians exposed to urban pluvial flooding. *Natural Hazards* **82**:1259–1278, 2016. https://doi.org/10.1007/s11069-016-2242-z

[16] Y. Wang, R. Marsooli. Physical instability of individuals exposed to storm-induced coastal flooding: Vulnerability of New Yorkers during Hurricane Sandy. *Water Resources Research* **57**(1):e2020WR028616, 2020. https://doi.org/10.1029/2020WR028616

[17] J. Xia, R. Falconer, Y. Wang, X. Xiao. New criterion for the stability of a human body in floodwaters. *Journal of Hydraulic Research* **52**(1):93–104, 2014. https://doi.org/10.1080/00221686.2013.875073

[18] M. Postacchini, G. Bernardini, M. D'Orazio, E. Quagliarini. Human stability during floods: Experimental tests on a physical model simulating human body. *Safety Science* **137**:105153, 2021. https://doi.org/10.1016/j.ssci.2020.105153

[19] C. Arrighi, H. Oumeraci, F. Castelli. Hydrodynamics of pedestrians' instability in floodwaters. *Hydrology and Earth System Sciences* **21**(1):515–531, 2017. https://doi.org/10.5194/hess-21-515-2017

[20] Q. Li, J. Xia, B. Dong, et al. Risk assessment of individuals exposed to urban floods. *International Journal of Disaster Risk Reduction* **88**:103599, 2023. https://doi.org/10.1016/j.ijdrr.2023.103599

[21] S. N. Jonkman, E. Penning-Rowsell. Human instability in flood flows. *JAWRA Journal of the American Water Resources Association* **44**(5):1208–1218, 2008. https://doi.org/10.1111/j.1752-1688.2008.00217.x

[22] J. Xia, Q. Chen, R. A. Falconer, et al. Stability criterion for people in floods for various slopes. *Proceedings of the Institution of Civil Engineers – Water Management* **169**(4):180–189, 2016. https://doi.org/10.1680/wama.14.00110

[23] E. Quagliarini, G. Romano, G. Bernardini. Investigating pedestrian behavioral patterns under different floodwater conditions: A video analysis on real flood evacuations. *Safety Science* **161**:106083, 2023. https://doi.org/10.1016/j.ssci.2023.106083

[24] X. Li, H. Yu, W. Song, et al. Fundamental diagrams for straight movement of pedestrians in water. *Safety Science* **159**:106018, 2023. https://doi.org/10.1016/j.ssci.2022.106018

[25] G. Bernardini, E. Quagliarini, M. D'Orazio, M. Brocchini. Towards the simulation of flood evacuation in urban scenarios: Experiments to estimate human motion speed in floodwaters. *Safety Science* **123**:104563, 2020. https://doi.org/10.1016/j.ssci.2019.104563

[26] T. Ishigaki, R. Kawanaka, Y. Onishi, et al. Assessment of safety on evacuating route during underground flooding. In *Advances in Water Resources and Hydraulic Engineering*, pp. 141–146. 2009. https://doi.org/10.1007/978-3-540-89465-0_27

[27] H. Lee, W. Hong, Y. Lee. Experimental study on the influence of water depth on the evacuation speed of elderly people in flood conditions. *International Journal of Disaster Risk Reduction* **39**:101198, 2019. https://doi.org/10.1016/j.ijdrr.2019.101198

[28] C. Dias, N. A. Rahman, A. Zaiter. Evacuation under flooded conditions: Experimental investigation of the influence of water depth on walking behaviors. *International Journal of Disaster Risk Reduction* **58**:102192, 2021. https://doi.org/10.1016/j.ijdrr.2021.102192

[29] State Administration for Market Supervision and Administration; State Administration for Standardisation. Human dimensions of Chinese adults. Tech. Rep. GB/T 10000-2023, State Administration for Market Supervision and Administration; State Administration for Standardisation, Beijing, 2024.

[30] M. Boltes, A. Seyfried, B. Steffen, A. Schadschneider. Automatic extraction of pedestrian trajectories from video recordings. In *Pedestrian and Evacuation Dynamics 2008*, pp. 43–54. 2010. https://doi.org/10.1007/978-3-642-04504-2_3

[31] S. P. Hoogendoorn, W. Daamen. Pedestrian behavior at bottlenecks. *Transportation Science* **39**(2):147–159, 2005. https://doi.org/10.1287/trsc.1040.0102

[32] A. Chevutschi, M. Alberty, G. Lensel, et al. Comparison of maximal and spontaneous speeds during walking on dry land and water. *Gait & Posture* **29**(3):403–407, 2009. https://doi.org/10.1016/j.gaitpost.2008.10.059

[33] S. Cao, J. Zhang, W. Song, et al. The stepping behavior analysis of pedestrians from different age groups via a single-file experiment. *Journal of Statistical Mechanics: Theory and Experiment* **2018**:033402, 2018. https://doi.org/10.1088/1742-5468/aab04f

A. Appendices

A.1. Methods

A.1.1. Instantaneous speed

$$v_i(t) = \frac{1}{\Delta t}\sqrt{\left[x_i\left(t+\frac{\Delta t}{2}\right) - x_i\left(t-\frac{\Delta t}{2}\right)\right]^2 + \left[y_i\left(t+\frac{\Delta t}{2}\right) - y_i\left(t-\frac{\Delta t}{2}\right)\right]^2}, \tag{1}$$

where $x_i\,(t)$ and $y_i\,(t)$ denote the coordinates of pedestrian i at time t, and $\Delta\, t$ is the time interval, which is 0.4 s in this paper.

A.1.2. Specific flood force

The specific flood force, a critical parameter in flood characterization, is determined by both flood depth and flow velocity, as expressed in Eq. 3. The relationship between characteristic flood force M and pedestrian walking speed v_i (Eq. 3) is extensively applied in flood evacuation modeling. Furthermore, the minimum walking speed v_min under varying characteristic flood forces M serves as a conservative benchmark for assessing pedestrian evacuation speed in flood conditions [32].

$$M = \frac{Dv_f^2}{g} + \frac{D^2}{2}, \tag{2}$$

$$v_i = \begin{cases} v_i^*, & 0 \le M \le M^* \\ a \cdot M^b, & M^* \le M, \end{cases} \tag{3}$$

where M denotes the characteristic flood force per unit width [$\mathrm{m^3\,m^{-1}}$]; D is the water depth [m]; g represents gravitational acceleration [$\mathrm{m\,s^{-2}}$]; v_f is the flood flow velocity [$\mathrm{m\,s^{-1}}$], set to zero for the hydrostatic condition in this study, v_f=0; v_i is the pedestrian walking speed [$\mathrm{m\,s^{-1}}$]; v_i^* is the critical walking speed, which is 1.69 $\mathrm{m\,s^{-1}}$ in this study; M^* represents the critical flood force per unit width [$\mathrm{m^3\,s^{-1}}$] , typically ranging from 0 to 0.02 $\mathrm{m^3\,s^{-1}}$; a and b are coefficients for the fitted curve.

A.1.3. Lateral swaying

Analysis of the trajectory data (Figure 3) reveals pronounced lateral sway, particularly in water. Lateral body sway is essential for maintaining balance while walking, with stride frequency and step length serving as key determinants of pedestrian speed. Following the method developed by Cao et al. [33] we calculated the trajectory curvature to quantify lateral swaying amplitude, stride frequency, and step length. These parameters were derived from the periodic variation in curvature, as illustrated in Figure 13.

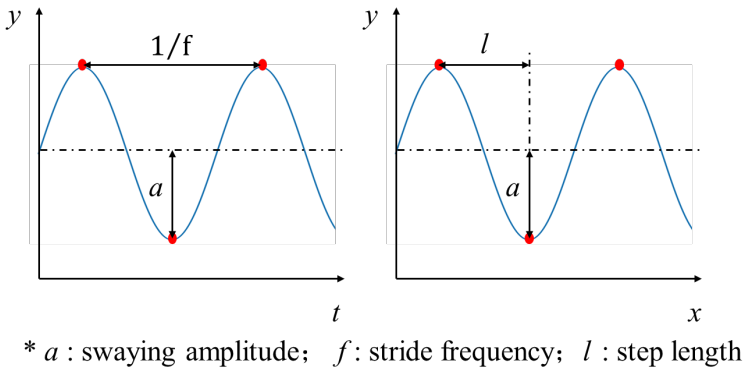


Figure 13. Schematic illustration of the sway amplitude (a), stride frequency (f) and step length (l).

A.1.4. Coefficient of variation (CV)

The CV is calculated using the following formula:

$$CV = \frac{\sigma}{\mu} \times 100\,\%, \tag{4}$$

where σ represents the standard deviation and μ denotes the mean.

A.2. Statistical analysis

A.2.1. Pearson correlation test between height, weight and pedestrian speed

	Variable			
	Height		Weight	
	Correlation coefficients r	p	Correlation coefficients r	p
0.35 m	0.216	0.0130	0.196	0.0243
0.60 m	0.386	0.0001	0.373	0.0002
0.90 m	0.220	0.0186	0.292	0.0016

Table 2. The results of Pearson correlation test between height, weight and pedestrian speed.

A.2.2. Statistical analysis of gender and water depth effects on speed

To examine the influence of gender and water depth on pedestrian speed, we first tested the normality of the data. Since speed distributions did not meet normality assumptions, the nonparametric *Kruskal–Wallis H-test* was applied, treating gender (male, female) and water depth (0 m, 0.35 m, 0.60 m, and 0.90 m) as a combined grouping factor. The analysis indicated a significant overall difference in speed among these groups ($\chi^2 = 308.95,\ \mathrm{DF} = 7,\ p < 0.001$), suggesting that both gender and water depth jointly affected pedestrian speed.

Influencing factor	Dependent variable	Chi-Square	DF	p
Gender×Water depth	Speed	308.95	7	<0.0001
Water depth	Female speed	123.97	3	<0.0001
Water depth	Male speed	164.87	3	<0.0001

Table 3. Nonparametric Kruskal-Wallis H test results on speed.

To further identify specific group differences, *Dunn's post-hoc test* was conducted. The results showed that gender had no significant effect on speed under dry conditions (0 m depth, $p = 1$), while significant gender differences emerged at all flooded depths ($p < 0.001$). This finding indicates that the influence of gender on walking speed becomes more pronounced in the presence of water, possibly due to differences in physical strength, stability, or adaptation strategies under resistance.

Influencing factor	Dependent variable	Z	p	Sig
Male, Female	Speed in 0 m water	−0.46	1	0
Male, Female	Speed in 0.35 m water	−3.29	0.02848	1
Male, Female	Speed in 0.60 m water	−4.82	<0.0001	1
Male, Female	Speed in 0.90 m water	4.06	0.00137	1

Table 4. Nonparametric Kruskal-Wallis H test results on speed.

A.2.3. Statistical analysis of water depth effect on swaying amplitude

Dunn's post-hoc test (Table 5) indicated no significant difference between swaying amplitudes at 0.35 m and 0.60 m depths, while significant differences were observed between all other depths.

	Z	p	Sig
0 m, 0.35 m	15.03783	<0.0001	1
0 m, 0.60 m	14.08831	<0.0001	1
0 m, 0.90 m	−7.03786	<0.0001	1
0.35 m, 0.60 m	−0.13401	1	0
0.35 m, 0.90 m	8.36548	<0.0001	1
0.60 m, 0.90 m	7.81562	<0.0001	1

Table 5. *Dunn's test* results of Water depth on Swaying amplitude.

A.2.4. Comparison with previous studies in Figure 6

Characteristics of the comparative data illustrated in Figure 6 are detailed in Table 6.

	Sample characteristics		**Sample dimension**		**Experimental site**
	Culture	**Age [years old]**	**Male**	**Female**	
This study	China	16∼33	101	87	swimming pool
Bernardini et al. [25]	Italy	5∼68	114	89	tank
Dias et al. [28]	Malaysia	22∼41	6	8	tank
Lee et al. [27]	Korea	20∼30	20	12	swimming pool

Table 6. The sample characteristics, and experimental site in Figure 6.

Similarly, the relationship between the minimum observed speed v_min, and the specific flood force (as shown in Table 7) was fitted.

	Parameters for the fitted curves	
	$\boldsymbol{v_i}$ $\boldsymbol{(a, b)}$	$\boldsymbol{v_{\min}}$ $\boldsymbol{(a, b)}$
This study	0.73, −0.11	0.48, −0.10
Bernardini et al. [25]	0.64, −0.09	−0.36, −0.13
Dias et al. [28]	0.66, −0.10	0.49, −0.12

Table 7. The parameters for the fitted curves in Figure 6.